Thammasat Int. J. Sc. Tech., Vol. 10, No. 2, April-June 2005

Extension of Ornstein-Zernike (OZ) Integral Equation to the Random Sequential Addition Model in Any Dimension

Panu Danwanichakul
Department of Chemical Engineering, Faculty of Engineering, Thammasat University
Klong Luang, Pathum Thani, 12120, Thailand.
E-mail: dpanu@engr.tu.ac.th

Abstract

Integral-equation theories of the Random Sequential Addition (RSA) model have been proposed in our previous work. It has been extensively studied as a two-dimensional problem representing an irreversible adsorption of large particles on a surface. This RSA model is, however, flexible enough to be applied to situations in other dimensions. It was used to model the growth of a polymer chain or a car-parking problem in one dimension and model a random sequential packing in three dimensions. We used the Fourier transform to solve the Ornstein-Zernike integral equation and its Percus-Yevick closure, both derived by utilizing the assumption of a binary mixture of quenched and annealed particles. In this work, we therefore applied the corresponding Fourier transform to one, two and three dimensions to compute the radial distribution functions, $g(r)$, and found that they are in good agreement with the results from Monte Carlo simulations. This confirms the validity of the theory.

Keywords: one dimension; two dimensions, three dimensions, random sequential adsorption, integral-equation theory, Ornstein-Zernike, Percus-Yevick

1. Introduction

The general description of the random sequential addition (RSA) model can be given as the following. To any D-dimensional space, particles are added one at a time randomly and remain at that position if they do not overlap with other particles previously added. If an overlap occurs the addition is rejected and a new attempt is made. The study of the probability of adding particles into available space in any dimension has been investigated after a seminal paper of Widom [1]. In that paper, the author showed that at low system densities, this model resulted in similar particle arrangements to ones in the equilibrium situation where all particles can move to their new positions in space all the time. The arrangements, however, differ at moderate and high densities. This finding brought RSA into attention as a model for an irreversible monolayer adsorption, where there are no surface diffusion and desorption detected during the time of experiment. The RSA, therefore, has been extensively applied to the study of adsorption which is a two-dimensional problem. It was found that RSA could well represent the adsorption of large molecules such as proteins [2] and colloidal particles [3] onto a solid surface, where the strong interaction between the particle and surface is comparatively greater than interactions among the particles themselves. The studies of RSA focus on kinetics of the deposition [4-6], in which the transport mechanism has to be incorporated in the model, and apply the equilibrium theory of liquid to non-equilibrium situations [7, 8].

Not only does the deposition of large molecules find an application in RSA, but certain experiments of atomic adsorption can also be described by this model. One example is the dissociative chemisorption of oxygen on Al (111) [9] which is also known as "hot deposition", and another is the early stages of simple catalytic reactions between CO and O_2 [10]. Still, the modification of RSA continues in order to explain more and more realistic situations.

In addition to the two-dimensional problems mentioned above, RSA was also applied to one-dimensional systems. Flory [11] utilized this model to study polymerization of vinyl monomers by means of statistics. That work was done using discrete sites for addition. Besides, the continuum version is popularly known as "the random car parking" problem [12], where many cars assumed as hard rods are put one by one at random on a line.

The application in a three-dimensional case is less popular than in any other dimensions since no realization in nature has been seen. Perhaps this could be a model in the study of packing of particles in a volume [13] akin to the well-known random close-packing used as a model for glass formation. Therefore, the study of RSA in three dimensions is rather theoretical and may contribute knowledge on structures of fluid and amorphous solids. However, the dynamics of RSA was already investigated in every dimension [14], including three dimensions.

It should also be mentioned that as in any other irreversible addition, RSA will finally lead to a jamming limit or car parking limit in 1D, at which no more additional particle can be added into the system since there is not available space to accommodate one more particle. These limits are quite interesting and closely related to the detail of the modification of the simple RSA. Typical 2D-RSA yields a jamming at a coverage of 0.547 [3]. Such limits have to be obtained by means of kinetics. We, however, are more interested in the structural problems which could be investigated through the integral-equation theories which we developed before for RSA [8]. In that work, we only studied two-dimensional problems. Thus, in this work we applied the model to one- and three-dimensional structures, which can be represented by the radial distribution function, $g(r)$. By definition, this function tells the probability of finding a particle in many distance r, far from a reference particle. In Section 2, we provided one of our theories, based on the binary-mixture approximation. Section 3 gives the details of numerical integration and the simulation method. Section 4 provides the results along with the discussion and Section 5 summarizes this paper.

2. Ornstein-Zernike Equation (OZ)

Integral equation theory was first used to study the structure of equilibrium liquids both in three and two dimensions, i.e. the monolayer film structure. In equilibrium situations, all particles move under the effects of other particles' interactions. However, there are some systems composed of moving particles in quenched structures such as a equilibrium, liquid in porous media. Madden and Glandt [15] and later Given and Stell [16] developed the application of integral equation theories to systems where at least one of the components is not in equilibrium, but quenched in an imposed configuration. The Replica Ornstein-Zernike (ROZ) integral equations [17], which are presented in the next section, have been applied to the description of fluids adsorbed within quenched disordered matrices. In a sequential quenching process, each newly arriving particle samples the space within the disordered matrix formed by the already quenched ones, and is thus a particular case of a quenched-annealed mixture. Even though process details of sequential quenching and RSA of hard spheres on a surface are different, surface diffusion is incorporated in sequential quenching but not in RSA, the final structures of the film grown through both models are equivalent, no matter whether each hard particle moves or not before it is quenched [8]. Thus, integral equation theory for sequential quenching can be directly applied to RSA of hard spherical particles. The hard sphere interparticle potential Φ is defined as a function of the center-to-center interparticle separation r, and with the particle diameter d:

$$\Phi(r)=\begin{cases}\infty & if\ r\le d\\ 0 & if\ r>d\end{cases} \qquad (1)$$

In the next subsection we give a brief explanation of equations used for adsorption within disordered matrices followed by the derivation of the integral equation for RSA based on a binary-mixture approximation.

2.1 Adsorption within Disordered Matrices

A fluid within in a disordered porous matrix can be viewed as a binary mixture of quenched particles (component 0) and equilibrated or annealed particles (component 1). Without loss of generality, we limit this presentation to systems with spherically symmetric interparticle forces. Let $\rho_{00}^{(2)}(r)$ denote the quenched structure's pair density function, let $g_{00}(r)=\rho_{00}^{(2)}(r)/\rho_0^2$ be its pair correlation function and let $h_{00}(r)=g_{00}(r)-1$ be the residual or total correlation function between two particles ("roots") separated by a fixed distance r. Similar correlations may be defined for 0-1 and 1-1 pairs. The Replica Ornstein-Zernike equations (ROZ) for such a system are:

$$\begin{aligned}
&h_{00}(r)=c_{00}(r)+\rho_0 c_{00}(r)\otimes h_{00}(r)\\
&h_{01}(r)=c_{01}(r)+\rho_0 c_{00}(r)\otimes h_{01}(r)+\rho_1 c_{01}(r)\otimes h_{c11}(r)\\
&h_{10}(r)=c_{10}(r)+\rho_0 c_{10}(r)\otimes h_{00}(r)+\rho_1 c_{c11}(r)\otimes h_{10}(r)\\
&h_{11}(r)=c_{11}(r)+\rho_0 c_{10}(r)\otimes h_{01}(r)+\rho_1 c_{c11}(r)\otimes h_{11}(r)\\
&\qquad +\rho_1 c_{b11}(r)\otimes h_{c11}(r)\\
&h_{c11}(r)=c_{c11}(r)+\rho_1 c_{c11}(r)\otimes h_{c11}(r)
\end{aligned}\tag{2}$$

where the symbol $\otimes$ denotes a convolution integral. The $c(r)$ in the above equations are the direct correlation functions, i.e. the sums of all coefficients ("diagrams" or "cluster integrals") in the density expansions of the corresponding total correlation functions $h(r)$ which are free from nodal points. These cluster integrals are best represented in graphical form; a review of graphical notation can be found in classical references [18]. The sub-indices c and b denote the so-called connected and blocking parts of the 1-1 correlations, distinguishing whether all paths between the roots in their graphical representation pass through a matrix particle or not.

2.2 Binary-Mixture Approximation

An evolving sequentially or differentially quenched system can be viewed as a binary mixture of the previously quenched particles (denoted by the index 0) and the (infinitely dilute) newly added particle(s) (denoted by 1), of number densities ρ and $d\rho$, respectively. In this approximation the instantaneous ROZ system (Eq. (2)) reduces to a single equation determining the equilibrium configuration of the annealed molecules prior to quenching:

$$h_{01}(r)=c_{01}(r)+\rho h_{00}(r)\otimes c_{01}(r)\,. \tag{3}$$

Equation (3) must be supplemented with an approximate closure such as the Percus-Yevick (PY) or any alternative. The PY closure for this quenched-annealed system is:

$$f(r)\left[1+h_{01}(r)\right]=c_{01}(r)\left[1+f(r)\right] \tag{4}$$

When the total density of the system increases from ρ to $\rho+d\rho$, a balance of particle pairs yields the change in the pair density function:

$$\begin{aligned}(\rho+d\rho)^2 g_{00}(r;\rho+d\rho)&=\rho^2 g_{00}(r;\rho)\\&\quad+2\rho\, d\rho\, g_{01}(r;\rho)\end{aligned}\tag{5}$$

The first term on the right-hand side represents the pre-existing pairs while the second corresponds to the additional 0-0 pairs created upon quenching of equilibrium particles. A term of order $(d\rho)^2$ has been neglected. Upon rearranging we get:

$$\frac{d\left(\rho^2 g_{00}(r;\rho)\right)}{d\rho}=2\rho g_{01}(r;\rho) \tag{6}$$

Equation (6) together with its initial condition:

$$g_{00}(r;\rho=0)=e^{-\beta\Phi(r)} \tag{7}$$

where $\beta=\frac{1}{kT}$, T is the temperature and k is Boltzmann's constant. $\Phi(r)$ is the pair interaction, which for this work is a hard sphere as in Eq. (1) and describes the evolution of a structure built through sequential quenching. Equation (3) and its closure, e.g. Eq. (4), must be solved for $g_{01}(r)$ at each density in order to compute $g_{00}(r)$ through integration of the differential equation.

This theory has been proven in two dimensions before [8, 19] and now we present the complete manipulation for other dimensions in the next sections. Another work on integral-equation theory of RSA, derived from the diagrammatic expansion [7], is also investigated in all dimensions. It could be a good asset for comparison.

3. Numerical Integration and Simulation Method

3.1 Numerical Integration

For computational purposes, it is necessary to approximate the system by a mixture of discrete species, corresponding to the stepwise addition of finite amounts of material. The correlation functions were discretized in ρ-space using $\Delta\rho$ =0.001. The cut-off distance, at which the correlation functions are expected to decay to unity, is chosen to be $r_{cut} = 6d$, where d is again a core diameter of a spherical particle. Both in real space (r-space) and Fourier space (k-space), 120 increments are used in the calculations. The details are as follows. The initial pair correlation function at infinite dilution is simply Eq. (7). The structure evolves as the density of the system increases, which we denote as ρ_i. On taking the Fourier transform of both sides of Eq. (3), we obtain an algebraic relation:

$$\tilde{c}_{01}(k;\rho_i) = \frac{\tilde{h}_{01}(k;\rho_i)}{1+\rho_i \tilde{h}_{00}(k;\rho_i)} \qquad (8)$$

Here, $\tilde{c}$ denotes the Fourier transform of function c. Several numerical methods can be used in Fourier transformation, including the method by Lado [20]. The one-dimensional Fourier and inverse Fourier transforms are given by:

$$\tilde{F}(k) = 2\int_0^\infty F(r)\cos(kr)dr\,, \qquad (9a)$$

$$F(r) = \frac{1}{\pi}\int_0^\infty \tilde{F}(k)\cos(kr)dk \qquad (9b)$$

The two-dimensional Fourier and inverse Fourier transforms are written as:

$$\tilde{F}(k) = 2\pi\int_0^\infty rF(r)J_0(kr)dr\,, \qquad (10a)$$

$$F(r) = \frac{1}{2\pi}\int_0^\infty k\tilde{F}(k)J_0(kr)dk \qquad (10b)$$

where J_0 is the Bessel function of the first kind. Lastly, the three-dimensional Fourier and inverse Fourier transforms are:

$$\tilde{F}(k) = \frac{4\pi}{k}\int_0^\infty rF(r)\sin(kr)dr \qquad (11a)$$

$$F(r) = \frac{1}{2\pi^2 r}\int_0^\infty k\tilde{F}(k)\sin(kr)dk \qquad (11b)$$

We solve for $g_{01}(r)$ from Eq. (6) and PY approximation (Eq. (4)) simultaneously, using a standard Picard iteration algorithm at successively larger values of the density, i.e. $\rho_{i+1} = \rho_i + \Delta\rho$, with $\Delta\rho$=0.001 for 3D, 0.0025 for 2D and 0.01 for 1D, all corresponding to the insertion of only one particle at one time in the simulation method. We have tried many sizes of $\Delta\rho$ and we found that they give very little differences. However, using bigger $\Delta\rho$ than we use in this study may lead to a false calculation because the effect of the term $(\Delta\rho)^2$ has been neglected as shown in Eq. (5). In case of large $\Delta\rho$, we have to use the full version of Eq. (5) and the whole set of OZ equations as written in Eq. (2). This case has also been investigated. Each result for $g_{01}(r)$ is used to compute the next $g_{00}(r)$ from Eq. (6), written in discretized form as Eq. (12) until the required density is reached.

$$g_{00}(r;\rho_{i+1}) = \frac{\rho_i^2 g_{00}(r;\rho_i) + 2\rho_i\Delta\rho g_{01}(r;\rho_i)}{\rho_{i+1}^2} \qquad (12)$$

3.2. Simulation Method

We performed Monte Carlo simulations to verify the accuracy of the numerical results from the Ornstein-Zernike equations. The calculation of the radial distribution function $g(r_i + \frac{\Delta r}{2})$ is, as customary, based on a histogram for small increments of width Δr. The averaged distribution function is then trivially obtained as the ratio between the number of pairs N_i collected from n configurations, at the separation ranging from r_i and $r_i + \Delta r$ from the average particle to the corresponding number in a system of ideal-gas or randomly placed particles. The function is calculated from Eq.

(13.1), (13.2) and (13.3) for one-, two- and three-dimensional systems, respectively.

$$g_{1D}(r_i+\frac{\Delta r}{2})=\frac{2N_i}{\Delta r\rho_{1D}Nn} \qquad (13.1)$$

$$g_{2D}(r_i+\frac{\Delta r}{2})=\frac{N_i}{\pi r_i\Delta r\rho_{2D}Nn} \qquad (13.2)$$

$$g_{3D}(r_i+\frac{\Delta r}{2})=\frac{N_i}{2\pi r_i^2\Delta r\rho_{3D}Nn} \qquad (13.3)$$

N is the total number of particle in the system and ρ is the number density of the system defined according to its dimension as the number of particles per length, area and volume for one-, two, and three- dimensional systems, respectively. The reduced density can be defined as $\rho_{1D}^*=\rho_{1D}d$, $\rho_{2D}^*=\rho_{2D}d^2$ and $\rho_{3D}^*=\rho_{3D}d^3$, where d is denoted before as the hard-core diameter of a sphere.

The details of the simulations are as the following. Particles were added one by one in a system whose size is 100*d* in one dimension, 20*d* x 20*d* in two dimensions or 10*d* x 10*d* x 10*d* in three dimensions. We have tried many system sizes in this study and found that the difference is very little. The small system sizes used here are acceptable regarding the interaction of particles which only comes from a repulsive hard core. However, a finite size effect has to be taken into account if the potential contains long-range interactions. For example, if the interaction is a Stockmayer potential which incorporates a dipole-dipole interaction in addition to a soft Lennard-Jones part, the size has to be bigger to cover the long range of the interaction.

The simulation began with adding a particle onto a simulated surface. If the added particle overlapped with previously quenched particles, it was removed and a new addition is attempted until the insertion was successful. We employed a periodic boundary condition and the minimum image convention, surrounding the primitive cell with a periodic lattice of identical cells, so that a particle interacts with all other particles in this infinite system. Our final results, averaged over at least 10000 realizations in 1D and over 1000 configurations in 2D and 3D, are presented in the following section.

4. Results and Discussion

4.1 RSA on a line (one-dimensional problem)

Figure 1 shows the numerical solutions and the simulation points at a reduced density of ρ^* = 0.50, 0.65 and 0.74, closer to the jamming or saturation limit, ρ_∞^* = 0.747 [1]. The jamming limit of RSA in 1D can be obtained analytically but for other dimensions, the jamming densities have to be estimated from the kinetic law written as:

$$\rho_\infty^* - \rho^*(t) \quad t^{-1/D}, \qquad (14)$$

where $\rho^*(t)$ is the density near jamming limit, t is the time and D is the corresponding dimension. The details of how to obtain this law can be found in Ref. [14]. As typically known in RSA study, the pair correlation function diverges logarithmically at contact at the jamming limit. The numerical solution shown in the figure fails to follow that behavior. In fact, the theoretical results do not show any anomalies at the saturation density. This finding is not surprising given that the PY approximation neglects the elementary diagrams required for the description of the close packing of annealed particles, and presumably, also of the jamming of quenched particles.

The distribution function $g(r)$ shows the first peak which represents the probability of finding a particle at contact with the reference particle and a small second peak displaying short-ranged order which is the characteristic of hard-sphere systems. The function finally decays at long distance where there show no correlations among particles. If we use any attractive potential, when comparing at the same density, the distribution would contain more number of peaks and the peaks should be higher than the case of hard spheres, since there would be a clustering of particle.

We also checked the result with Ref. [7] whose graph showed the first peak with the same height as ours, confirming consistency with our result. In Figure 1, the simulation result agrees very well with the theoretical result at the system density of 0.50 and the difference at contact is seen for a density of 0.65 while discrepancies both at contact and at the second peak are pronounced at a density of 0.74. The discrepancies are attributed to the PY approximation which neglects some terms whose numerical values are greater as the density increases.

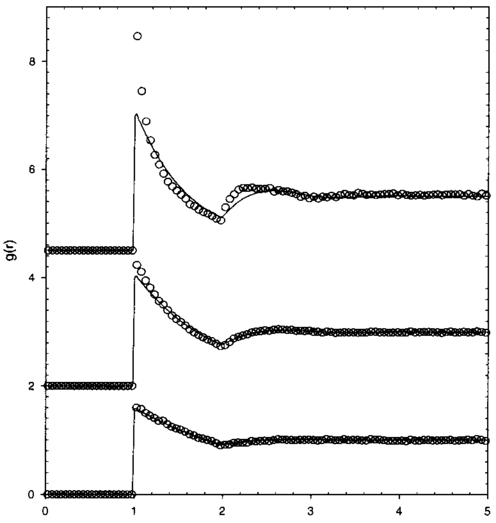

Fig. 1: The radial distribution function g(r) for the one-dimensional RSA for density of 0.50 (bottom), 0.65 (middle) and 0.74 (top). The bold line represents results from theory and circles are simulation results. For clarity, the top two curves were shifted.

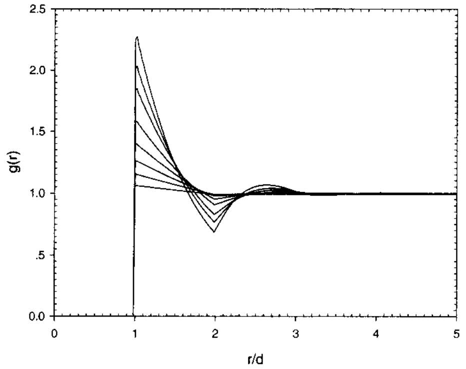

Fig. 2: The radial distribution function $g(r)$ from theory for the one-dimensional RSA at different densities, from 0.10, 0.20, 0.30, 0.40, 0.50, 0.60, 0.65, and 0.70 (lowest to highest first peaks)

Figure 2 compares g(r) at different temperatures ranging from density 0.10 to 0.70. The graph is more structured at higher density, showing higher first and second peaks because when the system gets denser, particles will be deposited at the position closer to one another. At the lowest density shown here, the function almost shows no correlation beyond the range of contact. The minima of all graphs are at the same position of $r = 2d$. This could be explained by imagining adding particles on a line one by one. A new particle will be added on either the right- or the left-handed side of the fixed particle. Since the particle is added at random, the probability for particles to be connected as a three-bead chain is the least. Particles will be deposited around the distance $2d$, but rarely at the exact position $2d$. This volume exclusion happens in the same way at every density, which is different from what happens in other dimensions as will be discussed in the next section.

4.2 RSA on a surface (two-dimensional problem)

As in the one-dimensional case, we show the comparison between simulation results and theoretical results in Figure 3. Both results are in good agreement at the density of 0.40 but the theory underestimates the value at contact at a density of 0.64, which is close to the jamming limit $\rho_\infty^* = 0.696$ [2]. The jamming limit in this case could be estimated by using the kinetic law (Eq. 14), but D is now equal to 2, corresponding to 2 dimensions.

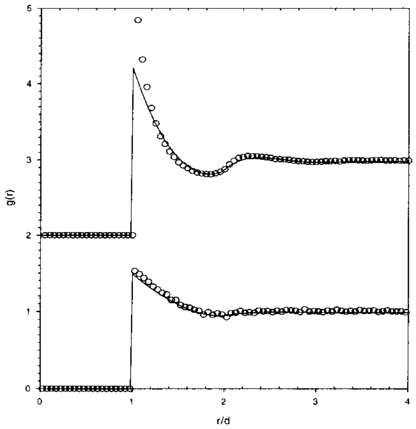

Fig. 3: The radial distribution function $g(r)$ for the two-dimensional RSA for density of 0.40 (bottom) and 0.64 (top). The bold line represents results from theory and circles are simulation results. For clarity, the top curve was shifted.

Figure 4 shows the comparison of $g(r)$ at various densities, ranging from 0.10 to 0.60. Again, featureless structure is seen at the lowest densities and disordered configurations generated through RSA are characterized by a weakly structured $g(r)$ at higher densities. As can be seen from the figure, the minima of the curves shift to the left when the density increases. This is not seen in one dimension. The least probable distances, which the particles are deposited far from the reference particle, is dependent on the density. At a very low density, the particles see each other as they are in one dimension so the minima is located near the distance $2d$. When the density increases, more particles will be added at the position around the reference particle. If particles can move in the system and the density is at the saturation density, the structure will finally develop to the triangular-crystalline structure of which the peaks of $g(r)$ will be at $r = d$, $1.732d$, $2d$ and so on. For this irreversible situation where particles cannot move, the volume exclusion will bring about the least probable distance shown in Figure 4 which gets closer to the value $1.732d$ as the density increases. It should also be noted that the second peaks of $g(r)$ in two dimensions are less obvious than in one dimension, showing that the structure in one dimension is more ordered than in two dimensions.

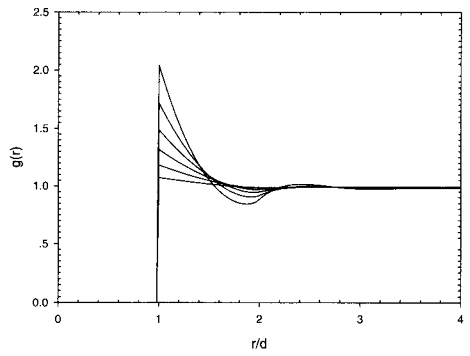

Fig. 4: The radial distribution function $g(r)$ from theory for the two-dimensional RSA at different densities, from 0.10, 0.20, 0.30, 0.40, 0.50 and 0.60 (the lowest to highest peaks).

4.3 RSA in a volume (three-dimensional problem)

RSA in three dimensions is studied along with other types of spherical packing in a volume. The distribution functions are shown in Figure 5 at the densities of 0.4 and 0.6, which is close to the jamming density $\rho_\infty^* \approx 0.735$ [13]. The kinetic law (Eq. 14) used to predict this limit in this case contains the parameter $D = 3$.

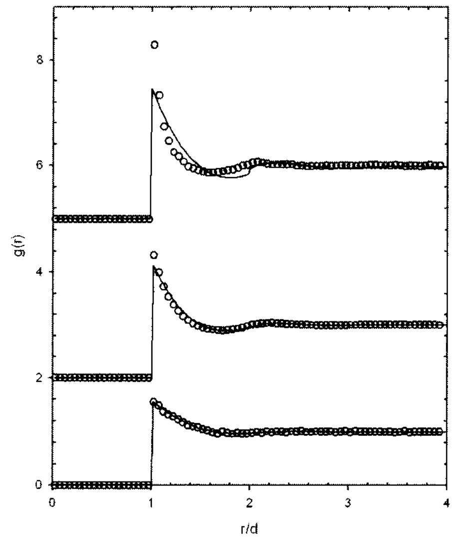

Fig. 5: The radial distribution function $g(r)$ for the three-dimensional RSA for density of 0.40 (bottom), 0.60 (middle) and 0.70 (top). The bold line represents results from theory and circles are simulation results. For clarity, the top curve was shifted.

The comparison between results from theory and simulation is very consistent at a density of 0.40 and they are much different at the densities of 0.60 and 0.74. Again the theory fails to report the correct values at contact for the density of 0.60 and both at contact and the second peak for the density of 0.74. These are due to the PY-approximation as already discussed. The short-range ordering can be seen at high density as shown in other dimensions.

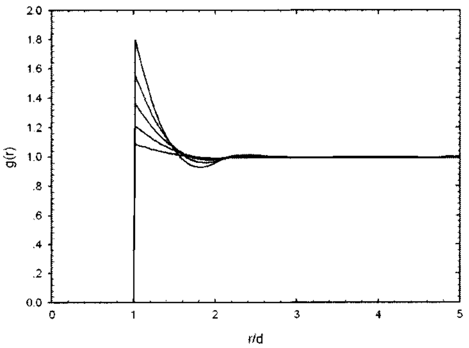

Fig. 6: The radial distribution function $g(r)$ from theory for the three-dimensional RSA at different densities, from 0.10, 0.20, 0.30, 0.40, and 0.50 (the lowest to highest peaks).

Figure 6 compares the function $g(r)$ at various densities ranging from 0.10 to 0.50 in three dimensions. This comparison is like ones in other dimensions, showing only short range correlations resulted from compact arrangements at high densities and uncorrelated structures at low densities. The minima of the curves shift to the left when the density increases, as in the case of two dimensions. If we consider the structure of the three-dimensional crystal, the peaks of g(r) will be at $r = 1d$, $1.632d$, $1.732d$, $2d$, and so on. In our systems of random sequential addition, both the irreversibility and exclusion effects cause the arrangement of particles to be disordered as also seen that the second peaks are not apparently formed.

5. Summary

The integral-equation theory or specifically, the modified Ornstein-Zernike equation for RSA, was first applied to the study of random sequential adsorption, a simple model for an irreversible deposition. Here, the theory has been adapted for other dimensions which may find applications in various fields ranging from chemistry, physics of liquids to biology. The dimensionality has been integrated into the theory by means of Fourier and inverse Fourier transforms which are essential tools for solving the equations. The results were shown, in every dimension, for various densities. The $g(r)$ at higher densities are more structured than at low density and they are consistent with the results from Monte Carlo simulations for the low and moderate system densities while they are quite different for the high densities. This is predictable since the integral equations were solved simultaneously with the PY-approximation which is poor at high density. We also checked our results with ones from a previous treatment in Ref. [7] and found good agreement. Even though the integral-equation theory underestimates the values at contact around jamming limits, it is, however, a method based on statistical mechanics which could provide clear understanding in terms of molecular interactions in the RSA process and other self-assemblies.

6. Acknowledgment

The author would like to express gratitude to Prof. Eduardo D. Glandt for background in statistical mechanics and for his guidance on the field.

7. References

[1] Widom, B., Random Sequential Addition of Hard Spheres to a Volume, J. Chem. Phys., Vol. 44, pp. 3888-3894, 1966.

[2] Feder, J. and Giaever, I., Adsorption of Ferritin, J. Colloid Interface Sci., Vol. 78, pp.144-154, 1980.

[3] Onoda, G. Y. and Liniger, E. G., Experimental Determination of the Random-Parking Limit in Two Dimensions, Phys. Rev. A, Vol. 33, pp.715, 1986

[4] Adamczyk, Z., B. Senger, J.-C. Voegal, and Schaaf, P., Irreversible Adsorption /Deposition Kinetics: A Generalized Approach, J. Chem. Phys., Vol. 110, pp. 3118-3128, 1999.

[5] Luthi, P. O., J. J. Ramsden and Chopard, B., Role of Diffusion in Irreversible Deposition, Phys. Rev. E, Vol. 55, pp. 3111-3115, 1997.

[6] Bafaluy, J., B. Senger, J.-C. Voegel, and Schaaf, P., Effect of Hydrodynamic Interactions on the Distribution of Adhering Brownian Particles, Phys. Rev. Lett., Vol. 70, pp. 623-626, 1993.

[7] Boyer, D., G. Tarjus, P. Viot and Talbot, J., Percus-Yevick Integral Equation for Random Sequential Addition, J. Chem. Phys., Vol. 103, pp. 1607-1613, 1995.

[8] Wang, Q., P. Danwanichakul and Glandt, E. D., Sequential Addition of Particles: Integral Equations, J. Chem. Phys., Vol. 112, pp. 6733-6738, 2001.

[9] Brune, H., J. Winttterlin, R. J. Behm, and Ertl G., Surface Migration of Hot Adatoms in the Course of Dissociative Chemisorption of Oxygen on Al (111), Phys. Rev. Lett., Vol. 68, pp. 624-626, 1992.
[10] Rampt, F. and Albano, V., Interplay Between Jamming and Percolation upon Random Sequential Adsorption of Competing Dimers and Monomers, Phys. Rev. E., Vol. 66, pp. 061106-1-6, 2002.
[11] Flory, P., Intramolecular Reaction Between Neighboring Substituents of Vinyl Polymers, J. Amer. Chem. Soc., Vol. 61, pp. 1518-1521, 1939.
[12] Bartelt, M. C., J. W. Evans, and Glasser, M. L., The Car-Parking Limit of Random Sequential Adsorption: Expansions in One Dimension, J. Chem. Phys., Vol. 99, pp.1438-1439, 1993.
[13] Cooper, D. W., Random-Sequential-Packing Simulations in Three Dimensions for Spheres, Phys. Rev. A, Vol. 38, pp. 522-524, 1988.
[14] Swendsen, R. H., Dynamics of Random Sequential Adsorption, Phys. Rev. A, Vol. 24, pp. 504-508, 1981.
[15] Madden, W. G. and Glandt, E. D., Fluid Distributions in Two-Phase Random Media: Arbitrary Matrices, J. Stat. Phys., Vol. 51, pp. 537, 1988.
[16] Given, J. A. and Stell, G., in Condensed Matter Theories, Vol. 8, edited by L. Blum and F.B. Malik, Plenum, New York, 1993.
[17] Given, J. A. and Stell, G., Comment on: Fluid Distributions in Two-Phase Random Media: Arbitrary Matrices, J. Chem. Phys., Vol. 97, pp. 4573-4574, 1992.
[18] Hansen, J. P. and McDonald, I. R., Theory of Simple Liquids, Academic Press, New York, 1986.
[19] Danwanichakul, P. and Glandt, E. D., Sequential Quenching of Square-Well Particles, J. Chem. Phys., Vol. 114, pp.1785-1790, 2001.
[20] Lado, F., Numerical Fourier Transforms in One, Two, and Three Dimensions for Liquid State Calculations, J. Comp. Phys., Vol. 8, pp. 417-433, 1971.